Korean J. Chem. Eng., **26**(6), 1813-1820 (2009)
DOI: 10.1007/s11814-009-0256-x

Preparation of molecularly imprinted polymer membrane with blending trimethoprim-MIP and polysulfone and its transport properties

Peimin Fan and Bing Wang†

Key Laboratory of Hollow Fiber Membrane Materials and Membrane Process of the Ministry of Education, School of Materials Science and Chemical Engineering, Tianjin Polytechnic University, Tianjin 300160, China
(*Received 3 October 2008 • accepted 8 April 2009*)

Abstract−An imprinted polymer membrane (IPM) with blending trimethoprim-MIP and polysulfone (PSF) was prepared by bulk polymerization and membrane preparation. In the process of the preparation, the influencing factors on membrane structure and properties, such as the concentration of PSF, the content of additive polyethelene glycol (PEG) and TMP imprinted polymer, were thoroughly investigated by scanning electron microscopy (SEM) and the membrane performance tester. The adsorption properties and selectivity properties of IPM to different substrates were estimated by using the method of equilibrium binding experiments. Finally, the transport properties of the membranes were investigated by using the diffusion chambers. The results showed that the imprinted polymer membrane exhibited a high selectivity for TMP.

Key words: Imprinted Polymer Membrane, Molecularly Imprinted Polymer, High Selectivity, SEM, Transport Properties

INTRODUCTION

Molecular imprinting is an attractive method of constructing the molecular recognition sites into the polymer matrix. As a result of its notable features, such as structure-activity predetermination, specific identification, broad applicability, strong anti-poor environment ability, good stability and long lifespan, the molecularly imprinted polymers (MIPs) have been widely used in many fields [1,2]. In particular, a considerable attention of the scientific community is being paid to the areas of drug separation [3] and biological sensors [4] using the imprinted polymer membrane prepared by this technique. However, during the preparation process of the imprinted polymer membrane, large amounts of cross linker are required in order to maintain the space configuration of the binding sites [5]. It also makes the imprinted polymer membranes have poorer flexibility and lower mechanical strength, which limits the practical application of the imprinted polymer membrane. Therefore, it is of great significance to develop a new method to make the imprinted polymer membrane not only have specific recognition but also have high flexibility so that they can be easily handled and used.

For the synthesis of a number of imprinted polymer membranes, the phase inversion technique has been used [6-10]. Despite their good recognition properties in aqueous media, these membranes were not stable in an organic environment, and the simultaneous formation of the pore structure and the binding sites in the phase inversion membranes became a significant limitation, since different optimal conditions were required [11]. Another approach for the synthesis of the imprinted polymer membranes was in situ cross-linking polymerization. The main problem with this approach was the high levels of cross-linking traditionally used in molecular imprinting for achieving a desirable selectivity, which made the imprinted polymer membranes have poor mechanical stability [12,13]. Moreover, for the approach in which plate membrane served as the supporting membrane, molecular template polymer was coated on the surface where the imprinted polymer membrane was prepared [14]. However, the interaction between the polymer and the supporting membrane usually depended on weak intermolecular forces. After repetitive using, polymer fell off from the supporting membrane, and the membrane no longer had selectivity.

In this work, the molecular recognition blend membrane was prepared by blending PSF and the template polymer at ratio, and the membrane not only had good specific recognition, but also kept fine flexibility and strength of the polysulfone membrane's own. It not only solved the problems of the instability of the phase inversion membranes in organic environment and the limitation to simultaneous formation of the pore structure and binding sites in the phase inversion membranes, but also overcame the problem of easy peeling by coating method. Thus, it provided a new experimental result for the practical application of the molecular recognition membrane.

EXPERIMENTAL

1. Materials

Trimethoprim (TMP), cephalexin, sulfadiazine were of analytical grade available from Beijing Bailingwei Co., Ltd. Methacrylic acid (MAA) was obtained from Tianjin Chemical Reagent Research Institute and purified by vacuum distillation to remove inhibitor before use. 2,2-Azo-bis-isobutyronitrile (AIBN) was of chemical grade and purchased from Shanghai Hewei Co., Ltd. Glycol methacrylate (GDMA) was of analytical grade and purchased from Beijing Bailingwei Co., Ltd. N, N-dimethylformamide (DMF) was available from Tianjin Chemical Reagent Co., Ltd. Polysulfone (PSF) was used as received from Motian Company of Tianjin Polytechnic University. Polyethelene glycol (PEG average Mw 600) was

†To whom correspondence should be addressed.
E-mail: bingwang666@yahoo.com.cn

obtained from Shanghai Synthesis Scour II Co., Ltd.

2. Instruments

All UV-vis spectra and adsorption experiments were performed with an UV-240 Ultraviolet-visible spectrophotometer (Shimadzu, Japan). A scanning electron microscope (SEM) (QUANTA-200) (FEI Co., Netherlands) was used to observe the morphology of the imprinted polymer membrane. To synthesize, prepare and process the products, there was some other equipment used: WE-1 thermostat water bath oscillator (Tianjin Honour Instruments Inc., China), SK5200 ultrasonic vibration generator (Shanghai Kudos Ultrasonic Instrument Co., Ltd., China), TG16-WS(1650D) supercentrifuge (Shanghai Luxiangyi Gentrifuge Instrument Co., Ltd., China.), long-wave (365 nm) ultraviolent lamp (Tianjin Amethyst/Zijin Special photo Source Co., Ltd.), Soxhlet extractor, etc.

3. Preparation of the Drug (TMP) Imprinted Polymer

The template TMP 0.0363 g (0.125 mmol) and the functional monomer MAA 0.04 ml (0.5 mmol) were dissolved in DMF (0.3 ml) with shaking for 4 h to form homogeneous solution, then the cross linker GDMA 0.47 ml (2.5 mmol) and the free radical initiator AIBN (2 mg) were added into the solution in turns. The solution was deoxygenated with nitrogen gas for 5 min, and nitrogen gas was removed under vacuum for 10 min. Then, the mixture was spread on the glass surface, and the glass was put into a quartz glass dish. To complete polymerization, the quartz glass dish was exposed to UV-light (λ=365 nm) under the protection of nitrogen gas for 6 h. The resultant rigid polymers were ground to pass through a 200 mesh sieve. Fine particles were removed by decantation in acetone. The resulting particles were placed in a soxhlet extractor and washed with 10 vol% acetic acid-methanol solution until the template could no longer be detected in the elution. Then, the particles were washed with pure methanol to remove the residual acetic acid and dried to constant weight under vacuum at 80 °C. As a control, the non-imprinted polymers (NIPs) in the absence of the template were prepared and treated by the same method.

4. Preparation of the Imprinted Polymer Membrane

Dry polysulfone 5.64 g was dissolved in 20 ml DMF as casting solution. That was followed by addition of 8.46 g MIP powder and 2.82 g PEG 600 additive to the casting solution, and stirred with a constant speed at 40 °C to prepare the blending solution. The solution would be placed under vacuum about 1 h to remove air bubbles. After air bubbles were removed completely, the solution was coated on a type of 20×20 cm glass surface at room temperature, then the plate membrane was prepared by using a scraper. Ten seconds later, this membrane was immersed into distilled water, and the imprinted polymer membrane with blending trimethoprim-MIP and polysulfone was obtained. Then the membrane was preserved in 50 vol% glycerol.

During the procedure of preparation of the blend membrane, a casting solution with different concentrations of PSF and PEG was used to optimize the composition of the blend membrane.

5. Analysis of the SEM

For SEM observation, the membrane samples were immersed into 50 vol% glycerol for 24 h, then taken out to wipe away glycerol on the surface and were dried at room temperature. After dehydration, desiccation, fixing and gold spraying, a scanning electron microscope (QUANTA-200) was used for the morphology observation of the surface and section of the membrane.

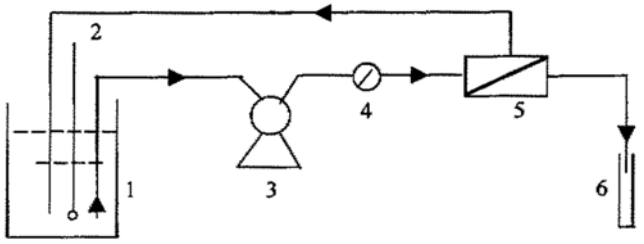

Fig. 1. Membrane performance tester.

6. Test of Mechanical Property of the Imprinted Polymer Membrane

Mechanical property measurement of the imprinted polymer membrane was performed with a Fabric Strength Tester (Y(TCB) 026H-500). The type of sample was 20 cm×5 cm, and stretching rate was 100 mm/min.

7. Test of Membrane Structure

The experiment was conducted by using the self-made membrane performance tester from the Membrane Separation Engineering Institute of Tianjin Polytechnic University, as shown in Fig. 1. At a set temperature, pure water was pumped from the reservoir to the plate membrane, and then flowed through the microporous plate membrane under certain pressure to the graduate finally. Through the determination of pure water flux in a certain time, the pure water flux in unit time was calculated. Furthermore, the pore size of membrane was calculated.

Where 1-6 represent the reservoir, thermometer, pump, pressure gauge, plate membrane and graduate, respectively.

7-1. Test of Water Flux

A water flux test was conducted with the apparatus shown in Fig. 1. Effective area of the membrane was 25.5 cm^2. Under a pressure of 0.1 MPa, after preloading for 1 h to keep the water flux stable, the water flux was determined. The water flux was calculated by Eq. (1).

$$f_w = \frac{V}{At} \tag{1}$$

Where f_w is the water permeable rate ($L/m^2 \cdot s$), V is the transmission liquid volume (L), A is the effective area of membrane (m^2) and t is the time (s).

7-2. Test of Porosity

The method of testing the quality difference between dry and wet membrane was used to determine the porosity of the membrane. The porosity was calculated according to Eq. (2):

$$\varepsilon = \frac{(W_1 - W_2)/d_{H_2O}}{V} \times 100\% \tag{2}$$

Where W_1 is the quality of wet membrane (g), W_2 is the quality of dry membrane (g), ε is the porosity of membrane, d_{H_2O} is the density of water (g/ml) and V is the apparent volume of membrane (ml).

7-3. Test of the Pore Size of Membrane

The pore size of the membrane was determined by the method of fluid permeability based on Poiseuille's law [15], and its basic principle is the Guerout-Elford-Ferry equation [16] derived from Poiseuille's law. The calculation of pore size is expressed by Eq. (3).

$$r = \sqrt{8\mu LQ/\varepsilon \Delta P} \quad (3)$$

Where r is the average pore size (m), ε is the porosity (%), L is the thickness of membrane (m), μ is the transmission liquid viscosity (Pa·s), Q is the water flow ($m^3/m^2 \cdot s$) and ΔP is the pressure differential between two sides of membrane (Pa).

8. The Binding Characteristics of Membranes

8-1. Binding Capacity of NIPM and IPM to TMP at Different Time

100 mg IPM (MIP content: 30 wt%) and 100 mg NIPM were placed, respectively, in the same concentration of TMP in the DMF solution (5 mmol/L). The equilibrium binding capacity of TMP was determined by Uv-vis spectrophotometry [17]. The experimental steps were as follows: the conical flasks which were filled with solutions were placed in a shaking bed, and oscillated several hours at room temperature. Then the solutions at different time were transferred to the centrifuge tubes. After 15 min high-speed centrifugation, supernatant liquor (3 ml) was injected in a 50 ml volumetric flask, and then diluted to the certain size with DMF solution. Under certain wavelength, Uv-vis spectrophotometry was used to determine the equilibrium concentration of TMP in solutions. According to the changes of the TMP concentration before and after adsorption, the binding amounts of IPM and NIPM to TMP could be calculated.

8-2. Binding Capacity of NIPM and IPM to TMP at Different Concentrations

In this process, the initial concentration of TMP varied in the scope of 0.5-5 mmol/L, and 100 mg IPM and 100 mg NIPM were added, respectively. The equilibrium binding capacity of TMP at different concentrations was determined by Uv-vis spectrophotometry.

9. Selectivity Test of NIPM and IPM to TMP and its Structural Analogues

TMP and its structural analogues (cephalexin, sulfadiazine) with similar antibacterial effect were elected as substrates to prepare the substrate solutions of the three drugs under a fixed concentration (5 mmol/L) in DMF. Then 100 mg NIPM and 100 mg IPM were added to the three substrate solutions, respectively. The binding capacities of the three substrates were determined by the equilibrium binding experiments above.

10. Membrane Transport Experiments

The membranes were mounted in a diffusion cell consisting of two stirred chambers of 10 ml volume. The analytes with certain concentration (5 mmol/L) in DMF solution were placed in the feeding chamber, and pure DMF solution was placed in the receiving chamber. The amount of the transported analytes was determined by spectrophotometry in 10 h. All transport experiments were conducted at room temperature.

RESULTS AND DISCUSSION

1. Effect of PSF Concentration on Membrane Structure and Properties

A crucial influencing factor on the properties and structure of the blend membrane is PSF concentration. With the increase of PSF concentration, the membrane surface will thicken, the interconnection degree among holes and the porosity will decrease, and the pore size will reduce. Besides, the formation of macroporous structure in membrane will weaken. For porous membrane, instantaneous liquid-liquid phase separation commonly occurs in different concentrations. But for casting solution of high concentration, the PSF concentration is high at the interface between the membrane and coagulation bath; therefore, a porous surface with lower porosity will be formed, and the water flux will be reduced. The asymmetric membrane, which is dense at the surface layer and porous at the bottom layer, is prepared by the method of the delayed liquid-liquid phase separation in solvent systems with bad intersolubility. The effect of PSF concentration on the properties and structure of blend membrane is quite obvious. With the increase of PSF concentration, the transport properties of membrane will be reduced.

As shown in Fig. 2, with the increase of PSF concentration, the pore size decreases, which is also concluded from the reducing water flux determined. When the PSF content is 20 wt%, a satisfactory pore size distribution is obtained, and the morphology of membrane

Table 1. Effect of concentration of PSF on blend membrane structure and properties*

PSF content (wt%)	Water flux ($L/m^2 \cdot h$)	Pore size (nm)	Porosity (%)
12	318.3	55.7	72.2
18	272.6	49.1	65.8
20	234.9	42.2	60.5
22	205.6	40.1	56.2
24	123.1	18.9	27.1

*Additive content: 10 wt%; Coagulation bath temperature: 25 °C; Casting solution temperature: 25 °C

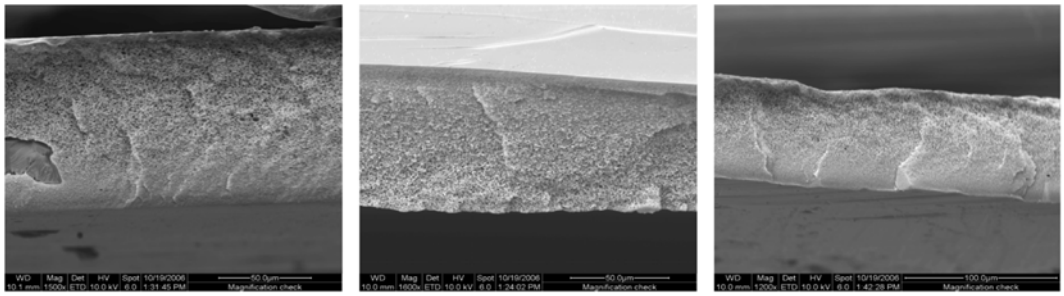

Fig. 2. SEM images of blend membrane with different content of PSF.

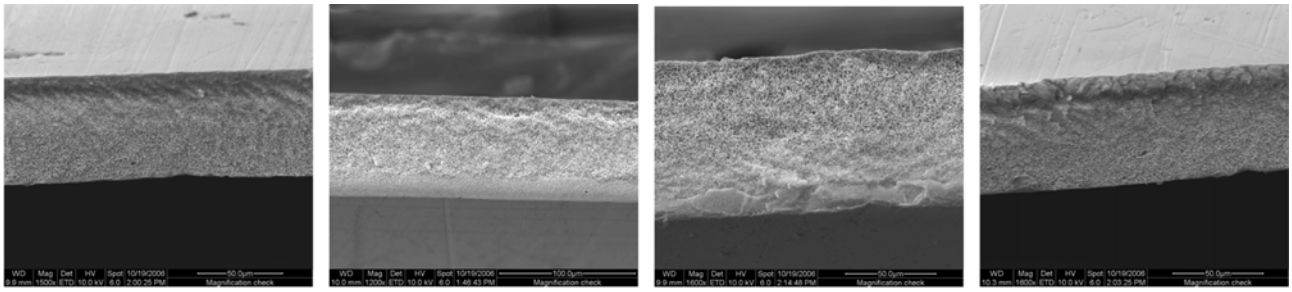

Fig. 3. SEM images of blend membrane with different content of PEG.

is good. Besides, it is clearly observed from Table 1 that with the increase of PSF concentration, the water flux reduces obviously, which is attributed to the decrease of pore size and porosity as a result of the increase of network density in membrane.

2. Effect of Content of PEG on Membrane Structure and Properties

To improve the structural morphologies and properties of the membrane, an additive is often added into the casting solution. Generally, the additive is a weak non-solvent of polymer, such as alcohols, acidic low molecular reagents, polymeric reagents (PVP, PEG etc.). The amount of additive should ensure the thermodynamic stability of casting solution and complete miscibility of system, because it can change the phase equilibrium relationship of membrane-forming systems; for instance, the homogeneous interval of the solution increases, the position of the initial composition in ternary phase diagram will be nearer to the liquid-liquid phase separation area, and the delayed liquid-liquid phase separation in the process of phase separation will transform into the instantaneous. As a result, a porous membrane with high porosity is formed. In the actual process of membrane preparation, macromolecule additives are often used to inhibit the formation of intramembrane large vacuoles and to improve the membrane porosity and the connectivity among holes. Besides, the existence of macromolecule additives not only increases the viscosity of casting solution but also inhibits the movement of polymer chains in casting solution.

Water-soluble additives not only affect the membrane structure by the position occupied in casting solution before the gelation process of membrane, but also affect the distribution of PSF in solution. The use of water-soluble additives can increase the affinity between the casting solution and precipitant, which can accelerate the non solvent diffusion speed, promote the phase separation of casting solution, and further influence the performance of the membranes. In this work, polyethylene glycol (PEG Mw 600) is elected as the additive, and the results are shown in Table 2.

The experimental results show that PEG is more than a pore-forming agent; its presence in casting solution can change the non solvent diffusion speed and promote or delay phase separation of casting solution, and further influence the performance of the membranes. With the increase of PEG content, the pore size and permeation rate increase obviously, whereas they significantly decrease when the content of PEG is more than 10%. Therefore, the content of additive PEG should be controlled in certain range in order to obtain membrane with better performance.

As shown in Fig. 3, with the increase of PEG content, the pore size increases gradually. But higher than 10 wt% of PEG content, the pore size decreases significantly, which can also be concluded from the decreasing permeation rate in Table 2. The results indicate that the increase of water flux depends on not only the increase of pore size but also the interconnection degree among pores.

3. Effect of Molecularly Imprinted Polymer on the Binding Capacities of the Membranes

After the imprinted polymer is added into the PSF membrane, the changes of morphology of the surface and section of the membrane are shown as Fig. 4 and Fig. 5. Also, Table 3 shows the absorption properties of NIPM and IPM to TMP in TMP solution (5 mmol/L).

As shown in Fig. 4 and Fig. 5, the prepared polymer membranes are asymmetric and opaque. The changes of adsorption capacities of NIPM and IPM to TMP at different time are shown in Table 3. Clearly, with the increase of binding time, the binding capacity of

Table 2. Effect of content of additive on blend membrane structure and properties*

Additive content (wt%)	Water flux ($L/m^2 \cdot h$)	Pore size (nm)	Porosity (%)
4	197	42.9	53.2
7	221	44.6	59.0
10	243	47.3	61.5
13	211	43.1	57.9

*PSF content: 20 wt%; Coagulation bath temperature: 25 °C; Casting solution temperature: 25 °C

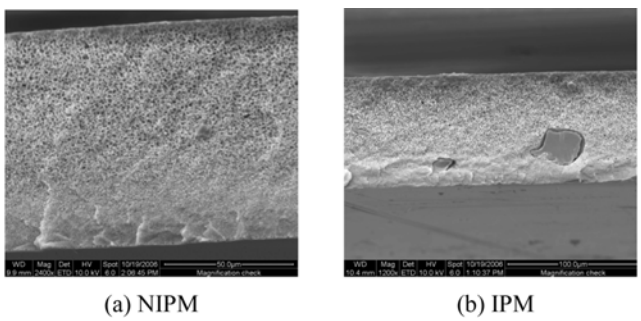

Fig. 4. Section configuration of NIPM and IPM.

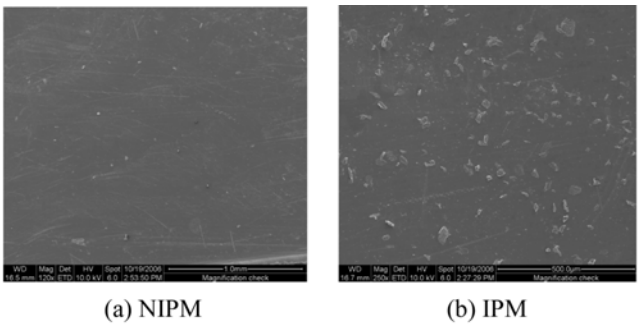

Fig. 5. Surface configuration of NIPM and IPM.

Table 3. Binding capacities of NIPM and IPM to TMP at different times

Time (h)	IPM (μmol/g)	NIPM (μmol/g)
3	65.2	7.3
6	86.9	7.4
9	97.7	7.3
12	103.4	7.4
15	103.9	7.4

IPM increases and then reaches an equilibrium value, but the binding capacity of NIPM remains basically unchanged. These results indicate that for the IPM, the TMP adsorption is caused by specific binding sites in the polymer membrane. When the solution containing TMP passes through the surface of IPM into the internal, TMP molecules are adsorbed by the binding sites. However, due to the absence of specific binding sites, NIPM is almost non-adsorptive to TMP molecules.

4. Binding Capacities of NIPM and IPM to TMP at Different Concentrations

In the experiments, the changes of the equilibrium binding capacities (marked as Q) of the polymer membranes to TMP were determined by the method of equilibrium binding experiments. As shown in Fig. 6, the binding capacity of NIPM to TMP is relatively small and increases along with the increase of TMP concentration, but for IPM, the binding capacity increases and then gradually reaches a larger equilibrium value. In many binding experiments of templates [18,19], because of the linear increasing of non-selectivity, the relation curve of the binding amount to the initial concentration is often difficult to reach the saturation point. So it could be learned that the adsorption of NIPM to TMP is non-selective, but the adsorption of IPM to TMP is selective. Comparing the synthesis processes of the two polymers, it could be inferred that the reason for selective binding of IPM to TMP is the formation of the specific recognition cavities complementary to the templates in shape and chemical functional groups. It also indicates that the interaction forces between template molecules and functional monomers in the preparation of the molecularly imprinted polymer play a very important role in the imprinted polymers' selectivity.

The Scatchard equation is commonly used for the evaluation of the binding characteristics of molecularly imprinted polymer to template molecules. The binding data of IPM to TMP were used for Scatchard analysis. The Scatchard Eq. (4) is as follows [20]:

$$Q/C_{(TMP)}=(Q_{max}-Q)/K_d \quad (4)$$

Where K_d (mmol/L) is the equilibrium dissociation constant of binding sites, Q_{max} (μmol/g) is the apparent maximal combination amount of binding sites, Q (μmol/g) is the binding amount of polymer to TMP, and $C_{(TMP)}$ (mmol/L) is the equilibrium concentration of TMP in solution.

According to the Scatchard equation, the relation curve between Q/C(TMP) and Q becomes almost straight, as shown in Fig. 7. The linear Eq. (5) is as follows:

$$Y=10.3-2x \quad (5)$$

The slope coefficient and intercept are $-1/Kd$ and Q_{max}/K_d respectively. It suggests that IPM forms a class of equivalent binding sites within the range of studied concentration, and exhibits uniform binding capacity to the TMP. The dissociation constant (K_d) and the apparent maximal combination amount (Q_{max}) of the IPM are calculated to be 0.5 mmol/L and 129 μmol/g, respectively. Q_{max} is far from the theoretical maximum combination capacity. This is mainly because, on the one hand, in the polymerization process, parts of TMP molecules are embedded, which makes them not to

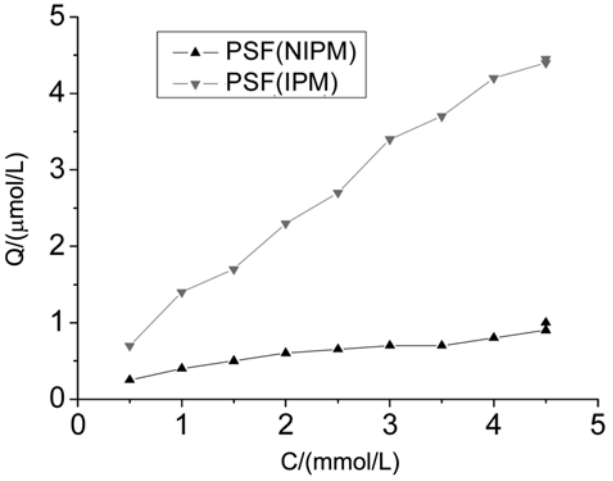

Fig. 6. Change curve of binding capacity along with different initial concentrations of TMP.

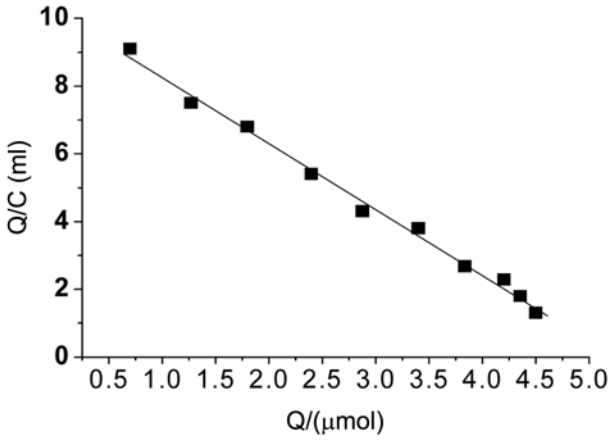

Fig. 7. Scatchard plot to estimate the binding nature of IPM.

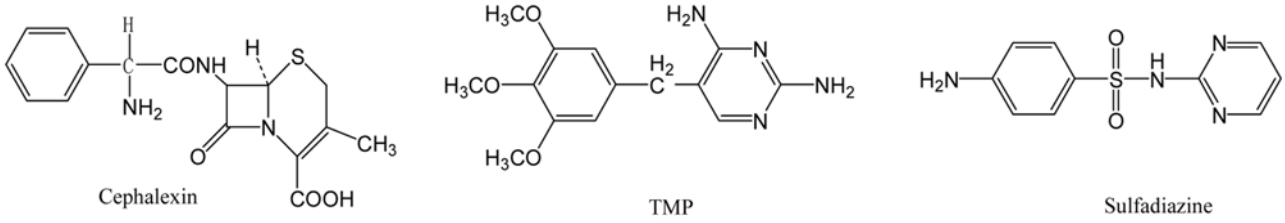

Fig. 8. Structural formulas of three substrates.

Table 4. K_D of the tested substrates on IPM and NIPM

Substrates	IPM			NIPM		
	C_P (μmol/g)	C_S (μmol/ml)	K_D (ml/g)	C_P (μmol/g)	C_S (μmol/ml)	K_D (ml/g)
TMP	133.81	4.21	31.78	30	5.61	5.35
Sulfadiazine	24.75	5.15	4.81	35.75	5.02	7.12
Cephalexin	20.83	5.84	3.57	21.62	5.81	3.72

be eluted cleanly; on the other hand, the solution used in the experiment is DMF, which has a strong polarity that it is not conducive to the formation of stable hydrogen bond between the template molecules and functional monomers. Therefore, it has a certain impact on the adsorption capacity of polymers. However, compared with the non-imprinted polymer membrane, the imprinted polymer membrane has higher adsorption to TMP, which indicates that the impact of solution on the adsorption capacity is not obvious.

5. Substrate Selectivity of IPM and NIPM

TMP and its structural analogues (cephalexin, sulfadiazine) with similar antibacterial effect were elected as substrates. The structural formulas of the three substrates are shown in Fig. 8.

The substrate solutions of the three drugs in DMF with the same concentration (5 mmol/L) were prepared, respectively. The distribution modulus K_D of the selected substrate between polymer membrane and solution was calculated according to Eq. (6) [21].

$$K_D=C_P/C_S \quad (6)$$

Where K_D is the distribution modulus (ml/g), C_P is the combinative concentration of imprinted polymer to substrate (μmol/g), and C_S is the equilibrium concentration of substrate in solution (μmol/ml).

After determination, the calculation data were shown in Table 4.

As can be seen from Table 4, compared with sulfadiazine and cephalexin, the IPM shows high selectivity for TMP, and compared with NIPM, the IPM has significantly greater binding capacity to TMP. But for sulfadiazine and cephalexin, the binding capacities of the two membranes to them were similar. Therefore, it could be deduced that the recognition to TMP of IPM may be attributed to the specific size/shape of recognition sites complementary to the template as well as correct position of the functional groups in the cavities involved in the template binding carboxyl. Although the NIPM and IPM have the same chemical composition, NIPM has no recognition sites complementary to the template molecule on shape and functional groups, and the carboxyl distribution in NIPM is arbitrary. Hence, its combination with substrates merely depends on the weak non-selective adsorption, which makes the selectivity greatly reduce.

6. Transport Properties of the Two Polymer Membranes

The shape of the template cavities and the functional groups arrangement of functional monomer in these cavities play important roles in the process of molecular recognition. The studies of the transport properties of the IPM can provide a deeper understanding of these roles. In this work, the transport properties of the IPM were investigated by using TMP, sulfadiazine and cephalexin as the analytes.

As shown in Fig. 9, the transfer rate of the TMP across NIPM is much slower than that across IPM, because of the existence of paths formed by cavities complementary to the template in specific size/shape as well as the correct position of the functional groups in IPM. However, there are none of these paths in NIPM, only irregular cavities are formed by pore-forming agent, and analytes could also pass through the irregular cavities but with lower transfer rate and no selectivity. As shown in Fig. 11, the transfer rates of all the analytes across the NIPM differ only slightly.

As shown in Fig. 10, compared with the TMP, the transfer rate of sulfadiazine across the IPM is faster. The reason is that the two drugs have similar structure, but the sulfadiazine is smaller than TMP, and there are no functional groups in the structural formula of sulfadi-

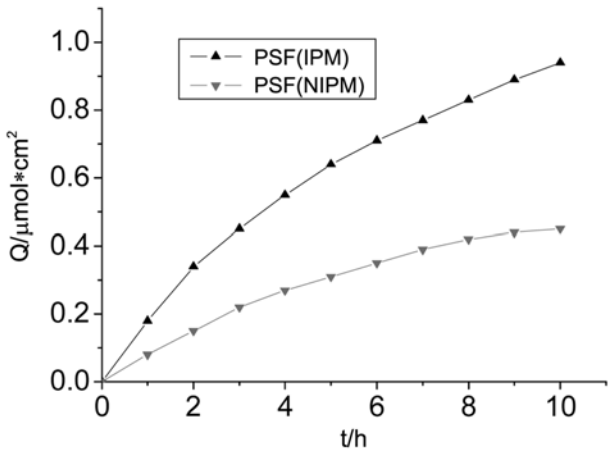

Fig. 9. The transferred amounts of the TMP across IPM and NIPM.

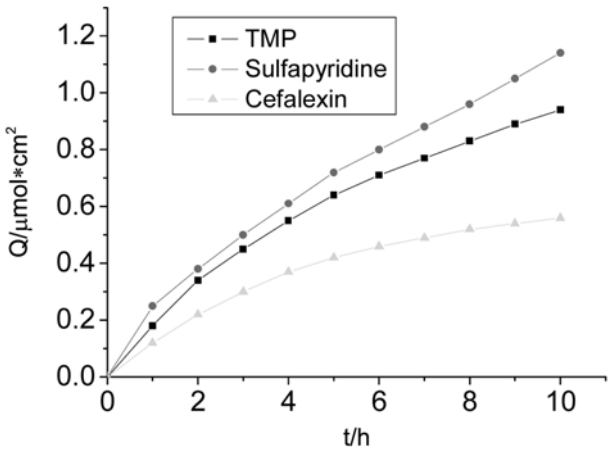

Fig. 10. The transferred amounts of the three analytes across IPM.

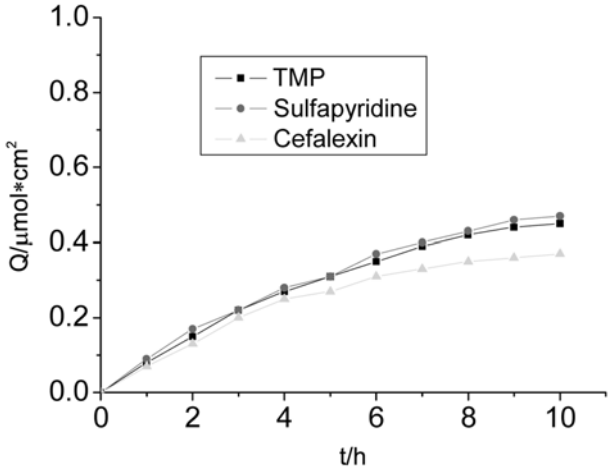

Fig. 11. The transferred amounts of the three analytes across NIPM.

azine forming the type of cooperative hydrogen bond with carboxyl. Considering that the IPM is imprinted with TMP, it is easy to understand that there is a specific size/shape of recognition sites complementary to the template TMP as well as correct position of the functional groups in the cavities involved in the template binding carboxyl. Therefore, TMP exhibits a stronger interaction with MAA in the IPM cavities than sulfadiazine, and the transfer rate of the TMP across the IPM is smaller compared with sulfadiazine.

To further testify if there are cavities in IPM matching the size of TMP, cephalexin which has a larger size than TMP is chosen as the analyte to transfer through the TMP imprinted polymer membrane. As shown in Fig. 10, compared with the TMP, the transfer rate of the cephalexin across the IPM is smaller, and this verifies that there are cavities in size/shape complementary to the template TMP.

The different transport properties of the imprinted and non-imprinted membranes could be attributed to the different polymer morphologies in polymerization with or without template molecules. The presence of template molecules during polymerization could result in a membrane having different structure, porosity and swelling compared with the corresponding non-imprinted membrane. The different size of the micropores and correct position of the functional groups in the imprinted and non-imprinted membranes lead to the differences in the transport properties of analytes.

7. Mechanical Properties of the IPM

The elongation at break and maximum load of IPM and NIPM were determined, respectively, in the experiment. The elongation at break and maximum load of NIPM are 25.5% and 11.4 N, respectively, and that of IPM are 23.3% and 9.97 N. Compared with NIPM, the elongation at break and maximum load of IPM decrease slightly; the possible reasons are that after MIP powders are added into the membrane, although physical crosslinking between MIP powder and macromolecular chain segments may be formed and limit the movement of molecular chain segments, the intermolecular forces between PSF macromolecule weaken. But, under these mechanical property parameters, it is sufficient enough to meet the need of the test for the adsorption and transport properties of IPM.

CONCLUSIONS

An imprinted polymer membrane with blending TMP-MIP and polysulfone was prepared. When the mass content of MIP, PSF and additive PEG was 30%, 20% and 10%, respectively, the blend membrane prepared exhibited good recognition ability to TMP as well as good flexibility and high mechanical strength. According to the Scatchard equation, the relation curve between $Q/C_{(TMP)}$ and Q became almost straight, and it could be learned that IPM existed a class of equivalent binding sites. Finally, the transport properties of the imprinted polymer membrane were investigated, which can provide a deeper understanding of the recognition mechanism of the imprinted polymer membrane in the process of molecular recognition.

ACKNOWLEDGMENT

The authors are indebted to the Natural Science Foundation of Tianjin for supporting this research. Contract grant number: 05YFJMJC04200.

REFERENCES

1. L. Ye, O. Ramström and K. Mosbach, *Anal. Chem.*, **70**, 2789 (1998).
2. Y. Jin, D.-K. Choi and K. H. Row, *Korean J. Chem. Eng.*, **25**, 816 (2008).
3. C. J. Percival, S. Stanley, M. Galle, A. Braithwaite, M. I. Newton, G. McHale and W. Hayes, *Anal. Chem*., **73**, 4225 (2001).
4. Q. Liu, Y. Zhou and Y. Liu, *Chin. J. Anal. Chem.*, **27**, 1341 (1999).
5. G. Wulff, A. Sarhan and K. Zabrocki, *Tetrahedron Lett.*, **44**, 4329 (1973).
6. M. Yoshikawa, J. Izumi and T. Kitao, *React. Funct. Polym.*, **42**, 93 (1999).
7. M. Yoshikawa, J. Izumi, M. D. Guiver and G. P. Robertson, *Macromol. Mater. Eng.*, **286**, 52 (2001).
8. H. Wang, T. Kobayashi, T. Fukaya and N. Fujii, *Langmuir*, **13**, 5396 (1997).
9. M. Ramamoorthy and M. Ulbricht, *J. Membr. Sci.*, **217**, 207 (2003).
10. R. Malaisamy and M. Ulbricht, *Sep. Purif. Technol.*, **39**, 211 (2004).
11. Y. Kondo and M. Yoshikawa, *Analyst*, **126**, 781 (2001).
12. S. Marx-Tibbon and I. Willner, *J. Chem. Soc., Chem. Commun.*, **10**, 1261 (1994).

13. S. Marx-Tibbon and I. Willner, *J. Am. Chem. Soc.*, **118**, 8154 (1996).
14. Z. Yang, Z. Xu and N. Bing, *Chem. Ind. Eng. Prog.*, **25**, 131 (2006).
15. X. He, G. He, B. Zeng, H. Sun, H. Yang, S. Chen and H. Zhou, *Journal of Xiamen University (Natural Science)*, **40**, 495 (2001).
16. Y. Zhang, *Technology of Water Treatment*, **27**, 99 (2001).
17. J. Zhou, X. He, W. Yang and H. Shi, *Chemical Journal of Chinese Universities*, **19**, 1388 (1998).
18. D. M. Hawkins, A. Trache, E. Ann Ellis, D. Stevenson, A. Holzenburg, G. A. Meininger and S. M. Reddy, *Biomacromolecules*, **7**, 2560 (2006).
19. Y. Jin and K. H. Row, *Korean J. Chem. Eng.*, **22**, 264 (2005).
20. I. Ferrer, F. Lanza, A. Tolokan, V. Horvath, B. Sellergren, G. Horvai and D. Barceló, *Anal. Chem.*, **72**, 3934 (2000).
21. D. Stevenson, *Trends in Ana1ytical Chemistry*, **18**, 154 (1999).